JOURNAL OF MAGNETIC RESONANCE 90, 464–473 (1990)

Improvements in Localized Proton NMR Spectroscopy of Human Brain. Water Suppression, Short Echo Times, and 1 ml Resolution

J. FRAHM, T. MICHAELIS, K. D. MERBOLDT, H. BRUHN, M. L. GYNGELL, AND W. HÄNICKE

Max-Planck-Institut für biophysikalische Chemie, Postfach 2841, D-3400 Göttingen, Federal Republic of Germany

Received April 9, 1990

Considerable technical improvements are reported for localized proton NMR spectroscopy using stimulated echoes. When compared to previous results, proton NMR spectra of the human brain are now obtainable (i) with *in vivo* water suppression factors of ≥ 1000, (ii) with only minor T_2 losses and negligible distortions due to J modulation at short echo times of 10–20 ms, and (iii) from volumes of interest as small as 1–8 ml within measuring times of 1–10 min. As a consequence, the detection of cerebral metabolites is greatly facilitated. This particularly applies to the assignment of those resonances (e.g., glutamate, taurine, inositols) that suffer from strong spin–spin coupling at the field strengths commonly in use for NMR in man. Studies of regional metabolite differences, tissue heterogeneity, and focal lesions in patients benefit from the increased spatial resolution and a concomitant reduction of partial volume effects. Localized proton NMR spectroscopy was performed on young healthy volunteers. Experiments were carried out on a 2.0 T whole-body MRI/MRS system using the standard headcoil for both imaging and spectroscopy.

Proton NMR spectroscopy of human brain *in vivo* finds increasing interest for both biological research and clinical applications. This is due to the high sensitivity of the proton, the abundance of metabolites accessible to proton NMR (*1, 2*), the dramatic spectral alterations observed in clinical pilot studies of cerebral tumors (*3, 4*) and infarction (*5, 6*), and the straightforward technical implementation in the form of an image-selectable localization module on commercial MRI systems. All these features particularly apply to the stimulated echo (STEAM) spectroscopy technique (*7–9*) since its one-shot localization capability has been proven to provide significant advantages in practical realizations.

Here we report on recent progress in the development of STEAM spectroscopy sequences that results in considerable improvements with respect to water suppression, short echo times, and small volumes of interest (VOI). In fact, with the present spatial, temporal, and spectral resolution, the metabolic access to the human brain is far beyond the feasibility studies performed only two to three years ago. Localized NMR spectroscopy clearly establishes itself as an indispensible, noninvasive tool for *in vivo* biochemical studies in man.

0022-2364/90 $3.00

METHODOLOGICAL ASPECTS

Figure 1 shows schematic diagrams of the STEAM spectroscopy sequence used for water-suppressed, localized proton NMR spectroscopy of the human brain. The principles of localization using stimulated echoes have been extensively described in earlier publications (*7–9*). The present sequence versions reduce the echo time TE to ≤20 ms and improve the effective water suppression by means of three successive CHESS pulses and associated spoiler gradients (Fig. 1a) that immediately precede the localization part of the STEAM sequence (Fig. 1b).

The efficiency of the water suppression was experimentally optimized on aqueous model solutions of cerebral metabolites. Using the final version of the water-suppressed STEAM sequence, the water resonance could be completely eliminated from single-

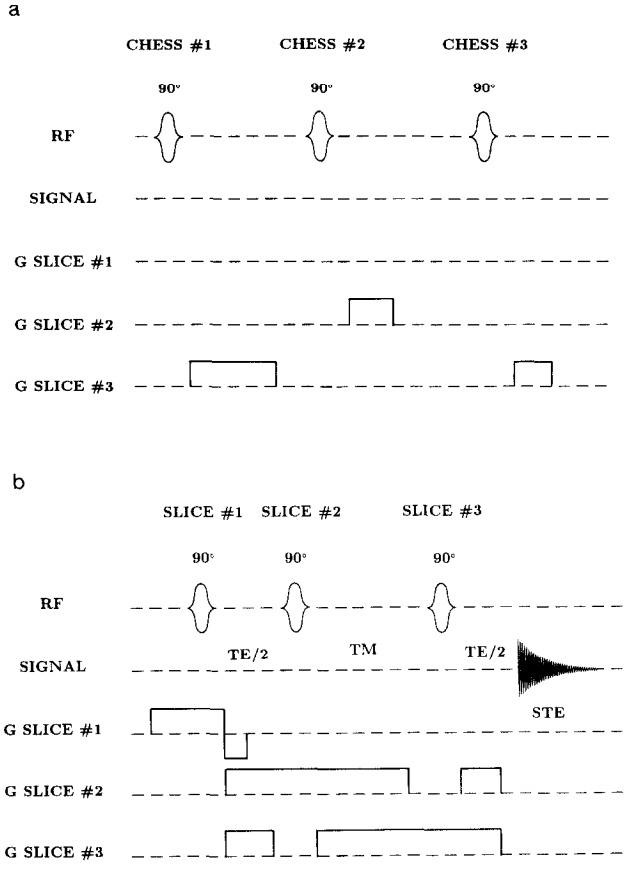

FIG. 1. Schematic diagrams of the radiofrequency and magnetic field gradient sequences used for water-suppressed, localized proton NMR spectroscopy *in vivo*: (a) water-suppression sequence and (b) subsequent STEAM localization sequence. Depending on the desired VOI sinc-shaped slice-selective RF pulses had a duration of either 2.56 ms (4–8 ml VOI) or 5.12 ms (1–2 ml VOI). Both slice-selection gradients and spoiler gradients for water suppression had a strength of 4 mT m^{-1}. Gaussian-shaped chemical-shift-selective (CHESS) RF pulses had a duration of 25.6 ms and a center-to-center distance of 110 ms. For further details see text.

scan, localized proton spectra (VOI = 8 ml, TE = 20 ms). The optimization started with one CHESS pulse (here CHESS 3) following the ideas of Moonen and van Zijl (*10*). However, instead of using first principles for the design of such delicate sequences, we found it more appropriate to develop the sequence step by step in order to account for practical imponderabilities. Consequently, the exact version described here only reflects the performance of our system. The resulting scheme must not be understood as a dogma but rather as a description of how to optimize in the presence of technical imperfections not present in theories.

In our case, three CHESS pulses were found to be necessary while four pulses gave no further improvement. CHESS pulses during the TM interval of the STEAM sequence were disregarded in order to keep the interval free for the inclusion of other spectral "editing" RF pulses (not described here) and to keep TM short to avoid motion/diffusion-induced signal attenuation caused by the necessary gradient pairs in the two TE/2 intervals. All CHESS pulses were Gaussian-shaped with a duration of 25.6 ms and a bandwidth of 60 Hz. They were applied to the same water resonance frequency with a time separation of 110 ms (center to center of the RF pulses). The corresponding spoiler gradients had a strength of 4 mT m^{-1}. The spoiler gradient following the final CHESS pulse (CHESS 3) of duration 20 ms (G SLICE 3) partially overlapped with the first slice-selection gradient (G SLICE 1) of the localization sequence (Fig. 1b). The durations of the first two spoiler gradients were 60 ms (G SLICE 3) and 30 ms (G SLICE 2), respectively. Their polarity was reversed with respect to that of all other gradient pulses in the same direction to keep their integral value close to zero. This strategy further reduced residual eddy-current effects and improved the long-term steady-state stability of the stimulated echo signal in multiple accumulations.

Slice-selective RF pulses in the localization part of the STEAM sequence were sinc-shaped with a duration of 2.56 ms. In all cases slice-selection gradient strengths were 4 mT m^{-1}. Gradient overlap during the TM = 30 ms interval was chosen to ensure efficient spoiling of unwanted coherences. For TE = 20 ms only slices 2 and 3 and for TE = 10 ms all three slices were refocused after the final RF pulse immediately before the acquisition of the stimulated echo. The latter scheme was chosen to avoid time-consuming gradient reversals and to enhance the spoiling capacity for the final unwanted FID. Data were acquired over an acquisition period of 1024 ms duration with a receiver bandwidth of ± 1 kHz. The first and third slice-selective RF pulse were synchronously phase cycled by 180° in alternate scans. Typically, the VOI ranged from 1–8 ml, i.e., $10 \times 10 \times 10$ to $20 \times 20 \times 20$ mm^3. For 1–2 ml acquisitions slice-selective RF pulses of 5.12 ms duration and an echo time of 20 ms were employed.

Proton NMR spectroscopy was performed on a 2.0 T whole-body MRI/MRS system (Siemens Magnetom) using the standard headcoil. Typical acquisition parameters were TR = 1500 ms (3000 ms), TE = 20 ms, and 256 (128) acquisitions keeping the measuring times to 6.5 min (13 min for 1–2 ml studies). Spectra were obtained by zero filling to 4K data points and a very mild Gaussian filtering of the time-domain data resulting in 0.2 Hz line broadening followed by Fourier transformation and zero- and first-order phase correction. No baseline correction, smoothing algorithms, or resolution enhancement was applied. All investigations were performed on healthy young volunteers (20–25 years old). Informed consent was obtained prior to the investigations.

RESULTS AND DISCUSSION

Water suppression. The primary aims of water suppression are to overcome the dynamic range problem of the analog-to-digital converter of the receiver channel and to avoid baseline problems due to an extended "foot" of the residual waterline. Both effects are sufficiently dealt with by using the present approach. Figure 2 shows typical water-suppressed proton NMR spectra of the human brain from a gray matter region in the insular area (Fig. 2a) and a white matter region in the frontal brain (Fig. 2b), respectively. Obviously, suppression ratios of at least a factor of 1000 are routinely observed in human brain *in vivo,* while a further tenfold reduction may be obtained in aqueous model solutions.

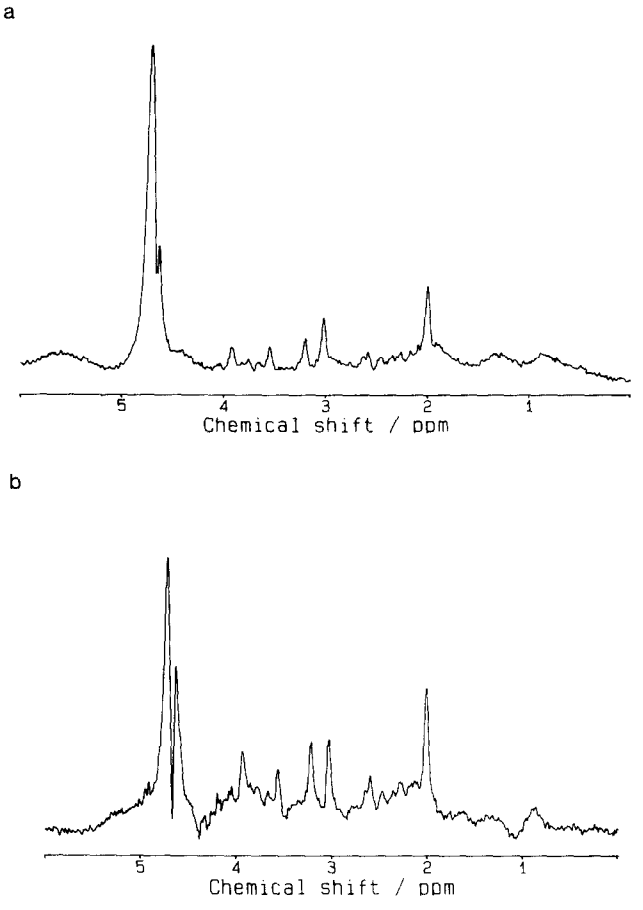

FIG. 2. Eighty-four megahertz (2.0 T) proton NMR spectra of an 8 ml VOI ($20 \times 20 \times 20$ mm^3, 256 acquisitions, TR = 1500 ms, TE = 20 ms, 0.2 Hz line broadening) of the adult human brain: (a) insular area (gray matter) and (b) frontal brain (white matter). The spectra demonstrate the routine quality of water suppression. The low signal ratio of choline (3.22 ppm) to creatine (3.03 ppm) in the insular area indicates a respectively lower choline concentration in gray matter than in white matter. Spectral intensities are scaled in proportion to the residual water resonance. For assignments see legend to Fig. 3.

Perhaps even more important is the clean baseline around the residual water resonance and the complete absence of spectral contamination or amplitude modulation outside a chemical-shift range of $\leq \pm 0.5$ ppm of the water resonance. Both effects are benefits of the Gaussian-shaped *excitation* of the water resonance frequency followed by gradient *dephasing* of the excited transverse magnetization. When technically available the excite–dephase water-suppression method is clearly superior to the use of binomial excitation or refocusing pulses.

The spectral resonances depicted in Fig. 2 are discussed in more detail in the subsequent section. Here, the spectra show the frequency range from 0 to 6 ppm with the chemical-shift scale being referenced to the CH_3 resonance (2.01 ppm) of *N*-acetyl aspartate (NAA). In general, proton brain spectra exhibit only very small signals from lipids (e.g., triglycerides) or from mobile side groups of cytosolic proteins. The tiny humps observed around 0.8 and 1.2 ppm represent typical findings in many regions of the brain when using echo times of $\leq$20 ms. Very low amplitudes are also found for the aromatic resonances of adenine nucleotides (7–8 ppm). However, spectral alterations in cerebral tumors and other pathologies may be accompanied by an increase of the lipid and/or aromatic resonances.

The differences in the creatine/choline ratio in gray (Fig. 2a) and white (Fig. 2b) matter regions reflect true differences in the respective metabolite concentrations. The relatively low choline concentration in gray matter becomes much more pronounced than in previous studies. This finding highlights the essential advantage of the use of a small VOI (8 ml versus 27–64 ml in Ref. (*2*)) that helps to minimize partial volume effects with surrounding white matter tissues.

Metabolic access at short echo times. Previous proton NMR studies at echo times of 50–270 ms (*2*) have revealed the importance of short echo times, i.e., echo times of $\leq$20 ms, to avoid spectral complications due to complex *J* modulation of spin–spin split resonances in the presence of strong coupling. These effects are frequently encountered at field strengths of 1.5–2.0 T and, e.g., apply to metabolite resonances of *N*-acetyl aspartate, glutamate, glutamine, γ-amino butyric acid, taurine, and inositols. Figure 3 shows a comparison of proton NMR spectra of human brain *in vivo* acquired at echo times of 10 ms (Fig. 3a) and 20 ms (Fig. 3b). As in the examples shown in Fig. 2, the spectra contain only minor, unidentified aliphatic proton signals from lipids or proteins and no aromatic resonances. Therefore, these and all following spectra have been prepared in exactly the same way: the signal amplitudes were normalized to account for different sizes of the VOI, and the frequency range was limited to 3 ppm in order to simplify the visual inspection of the excellent resolution between 1.2 and 4.2 ppm.

The spectra in Fig. 3 originate from an 8 ml VOI in the medioparietal cortex of the same volunteer and refer to almost exclusively white matter. They demonstrate that for both TE = 10 ms and TE = 20 ms only minor signal losses due to T_2 relaxation and negligible distortions due to *J* modulation of spin-coupled resonances are to be expected. In particular, the absence of complex modulation patterns of *strongly* coupled and potentially overlapping resonances from CH_2 groups of a variety of amino acids provides a major simplification for resonance assignments. These observations have been confirmed by localized studies on aqueous solutions of cerebral metabolites using the same STEAM sequence and the same whole-body system. A detailed description

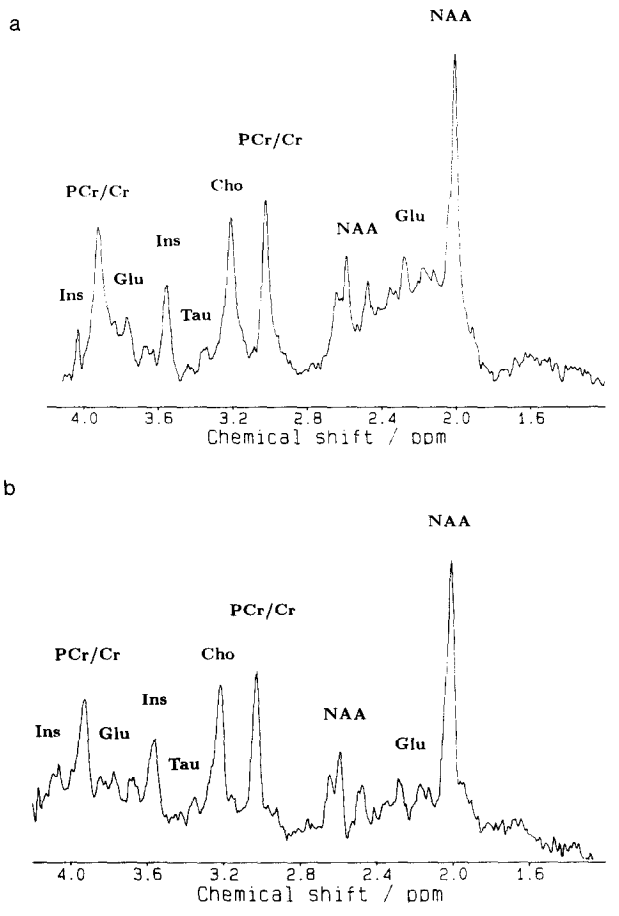

FIG. 3. Eighty-four megahertz (2.0 T) proton NMR spectra of an 8 ml VOI ($20 \times 20 \times 20$ mm^3, 256 acquisitions, TR = 1500 ms, 0.2 Hz line broadening) of the adult human brain localized in a medioparietal position of the cortex (white matter): (a) TE = 10 ms and (b) TE = 20 ms. The spectra demonstrate the capability of acquiring spectra at short echo times with only minor signal losses due to T_2 relaxation and negligible distortions due to J modulation of spin-coupled resonances. Resonances of the following metabolites have been identified: *N*-acetyl aspartate (NAA: 2.01 ppm, reference, 2.48, 2.60, and 2.64 ppm), glutamate (Glu: 2.11, 2.18, 2.28, 2.36, and 3.77 ppm), creatine (Cr) and phosphocreatine (PCr: 3.03 and 3.94 ppm), choline-containing compounds such as glycerophosphorylcholine (Cho: 3.22 ppm), taurine (Tau: 3.36 and 3.42 ppm, two further resonances below the choline peak), and inositol phosphates (Ins: 3.56, 3.64, 3.77, and 4.08 ppm).

of the metabolite assignments as well as of their correlation to *in vivo* spectra of human brain will be reported elsewhere.

On the basis of the spectral resolution presented here, it turns out that the signal ratio of the three strongly coupled aspartyl resonances (2.48, 2.60, and 2.64 ppm) of NAA to its *N*-acetyl resonance (2.01 ppm, reference) observed *in vivo* is very close to the corresponding ratio observed in aqueous NAA solutions (pH 7.1). This finding indicates that the entire CH_3 resonance must be attributed to NAA rather than to

other *N*-acetyl moities in the brain tissue. Moreover, similar experiments unambiguously demonstrate the absence of glutamine resonances from proton NMR spectra of the cortex in healthy adults. This finding is in agreement with the findings of recent analyses of brain tissue extracts (*11, 12*). The four strongly coupled resonances observed between the NAA resonances simply represent the spectrum of glutamate (Glu: 2.11, 2.18, 2.28, 2.36, and 3.77 ppm) under these experimental conditions (2.0 T, TE = 20 ms, TR = 1500 ms). Further assignments are made to creatine and phosphocreatine (PCr/Cr: 3.03 and 3.94 ppm), choline-containing compounds such as glycerophosphorylcholine (Cho: 3.22 ppm), taurine (Tau: 3.25, 3.31, 3.36, and 3.42 ppm, the first two resonances are covered by the choline peak), and inositol phosphates (Ins: 3.56, 3.64, 3.77, and 4.08 ppm). Cerebral lactate levels (CH_3 at 1.33 ppm) were generally below the level of detectability in healthy volunteers, but are quite often enhanced in focal lesions of patients after stroke or with malignant astrocytomas.

When comparing the spectra in Fig. 3, one observes that the TE = 10 ms spectrum is partially compromised by baseline distortions that are associated with the presence of strong coupling and spectral overlap as encountered in nonlocalized FID spectra of rat brain extracts at the same field strength (e.g., compare Ref. (*9*)). In general, the TE = 20 ms spectra exhibit a better definition of the baseline (2.0–2.6 ppm) without a penalty in signal-to-noise ratio (SNR) or *J* modulation. Another important advantage is the considerably increased spoiling capacity using crusher gradients after the final RF pulse of the localization sequence. For TE = 20 ms the approximately fourfold integral gradient power (8 ms gradient pulses) as compared to that for TE = 10 ms (2 ms gradient pulses) in the final TE/2 interval ensures the complete absence of signal contamination from regions outside the VOI even in critical locations, e.g., close to the skull. Since the reliability of spatial localization, i.e., the absence of partial volume effects, is a prerequisite for any meaningful application to patients, an echo time of 20 ms is considered to be preferable.

Temporal and spatial resolution. The temporal and spatial resolutions of localized *in vivo* NMR spectroscopy are of particular concern for the discrimination of small brain areas such as the pons or hippocampus, or when applications are extended from cooperative volunteers to the investigation of focal lesions in patients. A further argument in favor of a small VOI may be due to better shim capabilities in situations where the VOI can be placed *inside* a homogeneous part of the region of interest. Otherwise, the spectrum may be subject to susceptibility-induced line broadenings depending on the actual tissue environment. For example, a 4 ml ($16 \times 16 \times 16$ mm^3) VOI from the frontal part of the hippocampus may result in a better spectrum than an 8 ml ($20 \times 20 \times 20$ mm^3) VOI from the same location.

An illustration of the achievable trade-off between SNR, measuring time, and size of the VOI is given in Fig. 4. A twofold reduction of the VOI from 8 ml (compare Fig. 3b) to 4 ml with the measuring time kept constant (Fig. 4a) results in a loss in SNR similar to that for a fourfold reduction of the measuring time to 1.6 min with the VOI kept constant (Fig. 4b). It should be noted, however, that the spectra shown in Figs. 2–4 have been processed with only very mild filtering. An increase of the resulting line broadening from 0.2 to 0.5 Hz yields a remarkable improvement of the apparent SNR without a significant loss in spectral resolution.

The existence of tissue heterogeneity under both normal and pathological conditions

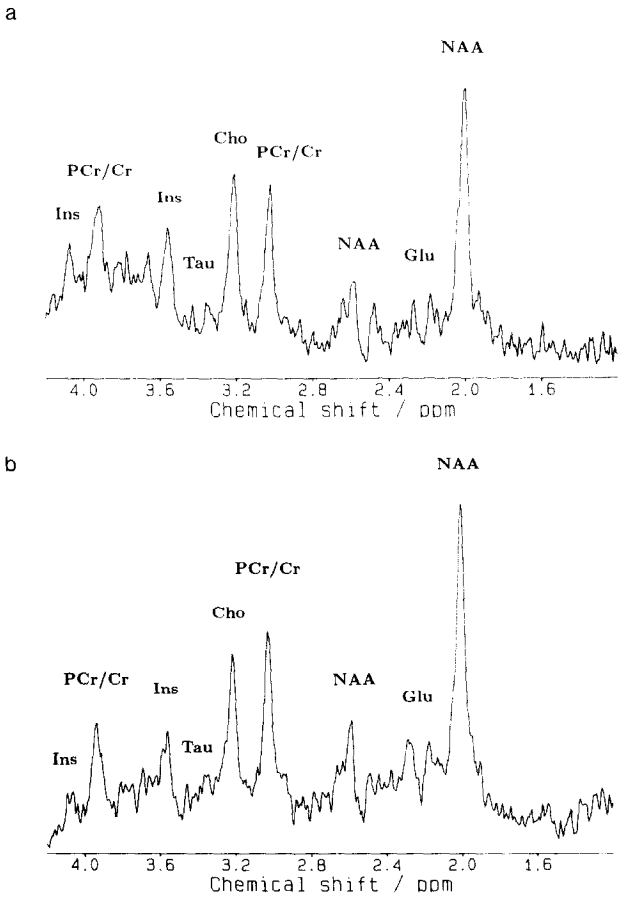

FIG. 4. Eighty-four megahertz (2.0 T) proton NMR spectra (TR = 1500 ms, TE = 20 ms, 0.2 Hz line broadening) of the adult human in a medioparietal positin of the cortex (white matter): (a) 4 ml VOI (16 × 16 × 16 mm^3), 256 acquisitions and (b) 8 ml VOI (20 × 20 × 20 mm^3), 64 acquisitions. The spectra demonstrate the possible trade-offs between signal-to-noise ratio, spatial resolution (4–8 ml), and temporal resolution (1.6–6.5 min) using the standard headcoil. For assignments see legend to Fig. 3.

often requires the use of the smallest possible VOI. Figure 5 therefore demonstrates our ability to acquire proton NMR spectra from a 1 ml VOI (TE = 20 ms, headcoil) in arbitrary locations within the human brain. Although the loss in SNR becomes obvious, the spectra allow an unambiguous assessment of the major metabolites NAA, PCr/Cr, Cho, and Ins as well as triglycerides and lactate if they are present in sufficient concentrations. Significant improvements are obtainable by increasing the VOI from 1 to 2 ml although the linear dimensions of the VOI need only to be increased from 10 to 12.6 mm. Such spectra have already been successfully recorded from small plaques in patients presenting with multiple sclerosis.

The concentration of NAA in the white matter of the cortex (Fig. 5a) is about a factor of 2 higher than that in the cerebellum (Fig. 5b). This interpretation is based on similar relaxation times for NAA in both regions (*2*). In general, the translation

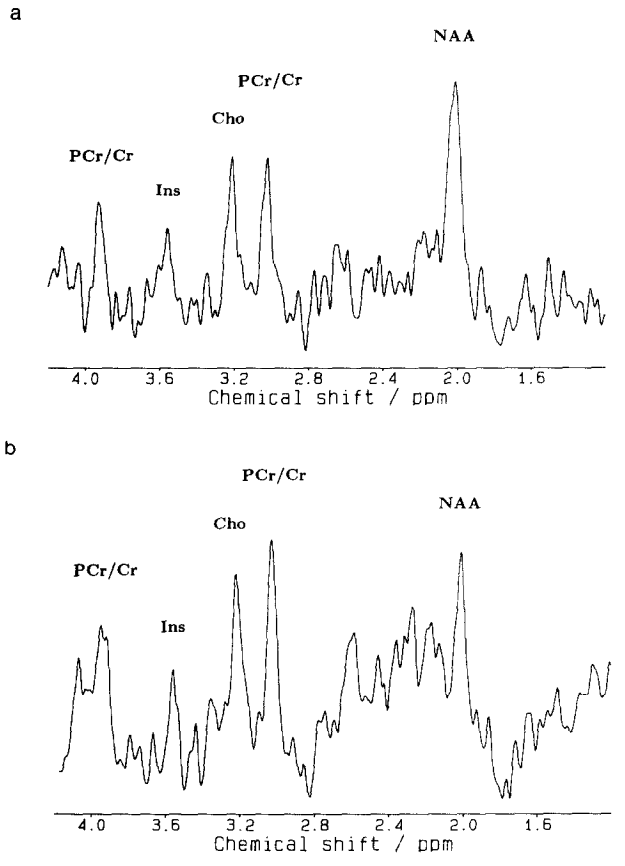

FIG. 5. Eighty-four megahertz (2.0 T) proton NMR spectra of a 1 ml VOI ($10 \times 10 \times 10$ mm^3, 512 acquisitions, TR = 1500 ms, TE = 20 ms, 0.5 Hz line broadening) of the adult human brain localized in (a) a medioparietal position of the cortex and (b) a midsagittal location of the cerebellum. Spectral differences in the NAA resonance reflect the corresponding metabolite concentration in white matter regions of the cortex and the cerebellum, respectively. For assignments see legend to Fig. 3.

of resonance intensities (peak areas) into relative metabolite concentrations is simplified with the use of short echo times due to a significant reduction of T_2 signal attenuation. In fact, most accessible cerebral metabolites exhibit relatively long T_2 relaxation times of the order of 100–500 ms *in vivo* (*2*). Saturation effects due to T_1 relaxation may be accounted for by acquiring spectra with two or more different repetition times, e.g., TR = 1500 and 3000 ms. A more detailed investigation of *in vivo* metabolite distributions in the normal human brain exploiting short echo times and small VOI sizes is in preparation. Attempts will be made to establish more reliable metabolite concentrations without the adverse effects of complex *J* modulation and partial volumes.

CONCLUSIONS

The spectral, temporal, and spatial resolution of localized proton NMR spectroscopy of the human brain *in vivo* has matured to such a degree that biochemical and phys-

iological studies of both volunteers and patients may significantly benefit from this noninvasive tool. The reliability of the spectroscopic results is emphasized by a high degree of intra- and interindividual reproducibility, at least in studies of healthy young volunteers. Future attempts will be made to more accurately quantify regional differences and to elucidate spectral alterations due to maturation and aging. Preliminary observations in patients confirm our expectations that clinical studies are remarkably improved by the increased spatial resolution and the concomitant reduction of partial volume effects as well as by the use of short echo times that result in much more discernable metabolic patterns or "fingerprints" due to an increased number of accessible metabolites.

ACKNOWLEDGMENT

Financial support by the Bundesminister für Forschung und Technologie (BMFT) of the Federal Republic of Germany (Grant 01 VF 8606/6) is gratefully acknowledged.

REFERENCES

1. J. W. PRICHARD AND R. G. SHULMAN, *Annu. Rev. Neurosci.* **9,** 61 (1986).
2. J. FRAHM, H. BRUHN, M. L. GYNGELL, K. D. MERBOLDT, W. HÄNICKE, AND R. SAUTER, *Magn. Reson. Med.* **11,** 47 (1989).
3. H. BRUHN, J. FRAHM, M. L. GYNGELL, K. D. MERBOLDT, W. HÄNICKE, R. SAUTER, AND C. HAMBURGER, *Radiology* **172,** 541 (1989).
4. C. M. SEGEBARTH, D. F. BALÉRIAUX, P. R. LUYTEN, AND J. A. DEN HOLLANDER, *Magn. Reson. Med.* **13,** 62 (1990).
5. H. BRUHN, J. FRAHM, M. L. GYNGELL, K. D. MERBOLDT, W. HÄNICKE, AND R. SAUTER, *Magn. Reson. Med.* **9,** 126 (1989).
6. P. C. VAN RIJEN, P. R. LUYTEN, J. A. DEN HOLLANDER, AND C. A. F. TULLEKEN, "Eighth Annual Meeting of the Society of Magnetic Resonance in Medicine, August 12–18, 1989, Amsterdam," p. 374.
7. J. FRAHM, K. D. MERBOLDT, AND W. HÄNICKE, *J. Magn. Reson.* **72,** 502 (1987).
8. J. FRAHM, H. BRUHN, M. L. GYNGELL, K. D. MERBOLDT, W. HÄNICKE, AND R. SAUTER, *Magn. Reson. Med.* **9,** 79 (1989).
9. J. FRAHM, T. MICHAELIS, K. D. MERBOLDT, W. HÄNICKE, M. L. GYNGELL, D. CHIEN, AND H. BRUHN, *NMR Biomed.* **2,** 188 (1989).
10. C. T. W. MOONEN AND P. C. M. VAN ZIJL, *J. Magn. Reson.* **88,** 28 (1990).
11. O. A. C. PETROFF, D. D. SPENCER, J. R. ALGER, AND J. W. PRICHARD, *Neurology* **39,** 1197 (1989).
12. J. PEELING, G. R. SUTHERLAND, AND J. GIRVIN, "Eighth Annual Meeting of the Society of Magnetic Resonance in Medicine, August 12–18, 1989, Amsterdam," p. 296.